Experimental infection of *Leishmania* (*Mundinia*) *martiniquensis* in BALB/c mice and Syrian golden hamsters

Nuchpicha Intakhan[1,2] • Wetpisit Chanmol[2] • Apisek Kongkaew[3] • Pradya Somboon[4] • Michelle D. Bates[5] • Paul A. Bates[5] • Narissara Jariyapan[4,6]

✉ Narissara Jariyapan

njariyapan@gmail.com

[1]Graduate PhD Degree Program in Parasitology, Faculty of Medicine, Chiang Mai University, Chiang Mai 50200, Thailand

[2]School of Allied Health Sciences, Walailak University, Nakhonsithammarat 80161, Thailand

[3]Animal House Unit, Faculty of Medicine, Chiang Mai University, Chiang Mai 50200, Thailand

[4]Department of Parasitology, Faculty of Medicine, Chiang Mai University, Chiang Mai 50200, Thailand

[5]Division of Biomedical and Life Sciences, Faculty of Health and Medicine, Lancaster University, UK

[6]Department of Parasitology, Faculty of Medicine, Chulalongkorn University, Bangkok 10330, Thailand

ABSTRACT

Our objective was to investigate clinical progression, presence of parasites and DNAs, parasite loads, and histological alterations in BALB/c mice and Syrian golden hamsters after intraperitoneal inoculation with *Leishmania* (*Mundinia*) *martiniquensis* promastigotes with a goal to choosing an appropriate animal model for visceral leishmaniasis. Infections were monitored for 16 weeks. Infected BALB/c mice were asymptomatic during the infection course. Parasite DNAs were detected in the liver at week 8 of infection, followed by clearance in most animals at week 16, whereas in the spleen parasite DNAs were detected until week 16. These results are correlated to those obtained measuring parasite loads in both organs. No parasite DNA and no alteration in the bone marrow were observed indicating that no dissemination occurred. These results suggest the control of visceralization of *L. martiniquensis* by BALB/c mice. In hamsters, weight loss, cachexia and fatigue were observed after week 11. *Leishmania martiniquensis* parasites were observed in tissue smears of the liver, spleen, and bone marrow

by week 16. Parasite loads correlated with those from the presence of parasites and DNAs in the examined tissues. Alterations in the liver with nuclear destruction and cytoplasmic degeneration of infected hepatocytes, presence of inflammatory infiltrates, necrosis of hepatocytes and changes in splenic architecture and reduction and deformation of white pulp in the spleen were noted. These results indicate a chronic form of visceral leishmaniasis indicating that the hamster is a suitable animal model for the study of pathological features of chronic visceral leishmaniasis caused by *L. martiniquensis*.

Keywords: *Leishmania martiniquensis* · *Mundinia* · BALB/c mouse · Syrian golden hamster · animal model

Introduction

Leishmaniasis is an infectious disease caused by protozoan parasites in the genus *Leishmania* and occurs in many tropical and sub-tropical regions of the world. Visceral leishmaniasis is one of clinical manifestations considered as the most severe, and frequently causes death if left untreated. The two main species responsible for symptomatic leishmaniasis-attributed fatalities are *L. donovani* and *L. infantum*. Other forms of leishmaniasis include cutaneous and mucocutaneous leishmaniasis (WHO 2019).

Various animal models have been used to elucidate pathogenesis, disease progression, drug treatment and immune responses to visceral leishmaniasis (Loría-Cervera and Andrade-Narváez 2014). Although several animals such as mice, hamsters, dogs, and non-human primates have been used in the study of leishmaniasis, the most widely used experimental models of visceral leishmaniasis are BALB/c mice and Syrian golden hamsters (Nieto et al. 2011).

Murine models are popular and widely used in several fields of biomedical research, including the study of visceral leishmaniasis, because of the large collection of inbred strains and ability to create transgenic animals (Nieto et al. 2011; Johnson 2012). Mice have been proved as a useful model animal to investigate and characterize immune mechanisms/responses and host factors that influence *Leishmania* infection, identify genes involved in infection, and also predict the functional role of those genes (Nieto et al. 2011; Ong et al. 2020). However, the clinical course of visceral leishmaniasis in BALB/c mice depends on several factors including *Leishmania* species, inoculum size, and inoculation route (Carrion et al. 2006; de Melo et al. 2020).

The Syrian golden hamster is highly susceptible to *L. donovani*, and *L. infantum*, and the clinicopathological features of the hamster model of visceral leishmaniasis closely mimic the human form of the disease. The infection presents with increasing visceral parasite burden, progressive cachexia, hepatosplenomegaly, pancytopenia, hypergammaglobulinemia and ultimately death (Loría-Cervera and Andrade-Narváez 2014). In several studies, hamsters have been used as a drug treatment model in the evaluation of efficacy of new compounds for both cutaneous leishmaniasis and visceral leishmaniasis (Robledo et al. 2012; Gupta et al. 2011).

In Thailand, most of leishmaniasis cases are caused by *L. martiniquensis* presenting as visceral and disseminated leishmaniasis (Leelayoova et al. 2017; Jariyapan et al. 2018). Animal models for the study of infectivity and pathogenesis of *L. martiniquensis* are needed. The clinical manifestations of an ideal animal model should resemble those occurring in humans, which present with weight loss, infection in internal organs such as liver, spleen, and bone marrow, and dissemination to the skin in the cases of immunocompromised hosts. Appropriate animal models would facilitate understanding of the biology of the parasite, clinical presentation and progression of the disease.

So far, a few studies regarding animal infection of *L. martiniquensis* have been reported (Garin et al. 2001; Somboonpoonpol 2016; Becvar et al. 2020). Garin et al (2001) have infected BALB/c mice with two strains of a presumed monoxenous trypanosomatid isolated from humans (MHOM/MQ/92/MARl from an HIV patient and MHOM/MQ/97/MAR2 from an immunocompetent patient) that are later identified as *L. martiniquensis* (Desbois et al. 2014). Both strains are infective to BALB/c mice after inoculation with promastigotes subcutaneously or intravenously and able to grow and disseminate in the popliteal and mesenteric lymph nodes, liver, spleen, and brain of the mice (Garin et al. 2001). However, differences of the kinetics of parasite burdens in the organs are observed according to the infective strain. Somboonpoonpol (2016) has revealed that *L. martiniquensis* (MHOM/TH/2011/PG) causes visceral disease in BALB/c mice when inoculated via intravenous and intraperitoneal routes, based on the presence of amastigotes and genomic DNA of the parasite in target organs. In another study, guinea pigs (*Cavia porcellus*) have been infected with *L. martiniquensis* (MHOM/MQ/1992/MAR1 and MHOM/TH/2011/CU1). The infected animals develop only temporary erythema lesion at the site of inoculation and no infection to sand flies (*Lutzomyia migonei*) is observed indicating that guinea pigs are not an appropriate model animal for studying *L. martiniquensis* (Becvar et al. 2020). In addition, based on

previous experience (Handman 2001), different strains of *L. martiniquensis* might be expected to cause different progression of visceral disease. Therefore, the current study was performed using a different strain of *L. martiniquensis* (MHOM/TH/2013/LSCM3) and to explore the possible use of hamsters as an alternative model. Infection and clinical progression of the disease was studied including presence of parasites and DNAs, parasite loads, and histological alterations of liver and spleen in both BALB/c mice and Syrian golden hamsters. The experimental data obtained from this study will help in determining an appropriate model for pathological study of visceral leishmaniasis caused by *L. martiniquensis*.

Materials and Methods

Animals and ethics statement

Male 8-10 week old BALB/c mice (*Mus musculus*) were purchased from Nomura Siam International Co., Ltd, Bangkok, Thailand. Male 8-10 week old Syrian golden hamsters (*Mesocricetus auratus*) were obtained from the animal house unit (in-house breeding) of the Faculty of Medicine, Chiang Mai University. All procedures performed on experimentally infected animals were reviewed and approved by the Ethics Committee on Animal Use of the Laboratory Animal Center, Chiang Mai University (Protocol number 2561/MC-0008).

Parasites

L. martiniquensis (MHOM/TH/2013/LSCM3) was used in this study (Chiewchanvit et al. 2015). Parasites were maintained in BALB/c mice for use in experimental infections as described below.

Preparation of promastigotes to infect animals

L. martiniquensis parasites used for experimental infections were isolated from the spleens of BALB/c mice previously inoculated intraperitoneally with *L. martiniquensis* promastigotes and maintained for 16 weeks. Briefly, an infected mouse spleen was collected aseptically and placed in a small volume of sterile phosphate buffer saline (PBS). The spleen was minced and strained using a cell strainer (SPL Life Sciences Co., Ltd., Gyeonggi-do, Korea) using aseptic techniques. The suspension was washed by centrifugation at 26 °C, 1,500 ×*g* for 10 min, the cell pellet resuspended in Schneider's insect medium (SIM) (Sigma-Aldrich, St. Louis, MO, USA) supplemented with 10% FBS and 25 μg/mL gentamicin

sulfate and cultured in the same medium at 26 °C without shaking. After 3-5 days of cultivation, promastigotes observed in the culture were subpassaged into RPMI-1640 medium supplemented with 20% FBS, pH 5.5, 25 μg/mL gentamicin sulfate to stimulate metacyclogenesis (Zakai et al. 1998). The resulting stationary phase promastigotes at day 5 of cultivation were used to infect animals.

Experimental infections

Eighteen BALB/c mice and 18 hamsters were used in this study. In each experiment, six animals were used as a control group and injected intraperitoneally with PBS. Twelve animals were intraperitoneally injected with 2×10^7 promastigotes of *L. martiniquensis* resuspended in 100 μl of PBS. The evolution of *L. martiniquensis* infection in BALB/c mice and hamsters was monitored weekly for clinical signs (weight loss, cachexia, fatigue, ascites, scabs or skin lesions, hepatomegaly, and splenomegaly) and their body weight recorded using a balance (Sartorious TE313S Talent Analytical Balance, Sartorius AG, Goettingen, Germany). At 8 and 16 weeks post infection, three animals from each control group and six animals from each infected group were sacrificed using isoflurane anesthesia. In each animal, the liver, spleen, and bone marrow were removed separately under sterile conditions. The liver and spleen were examined macroscopically and appearance recorded using a digital camera. Then, the liver and spleen samples were weighed and cut into several portions to examine for parasites using impression smears, culture, and histological analysis, and for detection of parasite DNAs using a PCR method (below). For bone marrow samples, only impression smears and PCR were performed.

Tissue impression smears

Tissue samples of the liver, spleen, and bone marrow from infected BALB/c mice and hamsters (8 and 16 weeks post infection) were smeared on glass slides. After air-drying, the smears were fixed with absolute methanol and stained with 5% (v/v) Giemsa's solution for 30 min. The stained smears were examined under a light microscope (Olympus America Inc., Center Valley, PA, USA) for amastigotes of *L. martiniquensis*.

Quantification of parasite loads by limiting dilution assay

Parasite loads in the liver and spleen of BALB/c mice and hamsters at 8 and 16 weeks post infection were quantified by limiting dilution assay (Buffet et al. 1995). Briefly, a piece of the infected liver or spleen was weighed on a precision balance and then minced in Schneider's insect medium supplemented with 10% FBS and 25 μg/mL gentamicin sulfate. The homogenates were strained using a cell strainer and washed in the medium by centrifugation at 26 °C, 1,500 ×*g* for 10 min. The supernatant medium was discarded. The pellet was resuspended in the same medium and dispensed in a 96 well microtiter culture plate (Nunc, Roskilde, Denmark). The suspension was five-fold serially diluted in the medium and incubated at 26 °C. The presence or absence of promastigotes in each well, which was examined daily for 14 days with an inverted light microscope (Olympus America Inc., Center Valley, PA, USA), was recorded. The parasite load was determined from mean of reciprocal positive titers (the last dilution containing promastigotes) divided by weight of homogenized cross section and calculated as the number of parasites per gram of organ.

Histological analysis

The liver and spleen of uninfected and infected BALB/c mice and hamsters at 8 and 16 weeks post infection were used for the histological analysis. Tissue samples of these organs were fixed in 10% buffered formalin solution and processed for embedding in paraffin. Tissue sections (5 mm) were cut using a microtome (Zeiss Hyrax M25, Oberkochen, Germany) and stained with Hematoxylin-Eosin (HE). The stained sections were examined under a light microscope (Olympus America Inc., Center Valley, PA, USA) to analyze histological alterations, cellular inflammatory infiltrates, and the presence of *L. martiniquensis* amastigotes in the organ tissues.

Detection of *L. martiniquensis* DNA by PCR

Total genomic DNA was extracted from tissues of the liver, spleen, and bone marrow of 8 and 16 weeks-infected BALB/c mice and hamsters using a genomic DNA purification kit (Thermo Fisher Scientific Inc., Waltham, MA, USA) according to the manufacturer's instructions. Parasite DNA was detected by amplification of *Leishmania* rRNA ITS-1 using the LeF/LeR primers (Spanakos et al. 2008). The PCR reaction mixture contained template DNA, 1×PCR reaction buffer (Invitrogen, Carlsbad, CA, USA), 4 mM $MgCl_2$ (Invitrogen, Carlsbad, CA, USA), 0.6 μM of each primer (Invitrogen, Carlsbad, CA, USA),

0.8 mM of each dNTPs (Invitrogen, Carlsbad, CA, USA), and 1U of Taq DNA polymerase (Invitrogen, Carlsbad, CA, USA). Amplification was performed in TPersonal Combi Thermocycler (Biometra, Göttingen, Germany) using a step of initial denaturation at 94 °C for 5 min, followed by 35 cycles of denaturation at 94 °C for 1 min, annealing at 65 °C for 1 min, extension at 72 °C for 2 min, and a final extension step at 72 °C for 5 min. Amplified products were run on 1.2% agarose gels (Amresco, Atlanta, GA, USA) containing ethidium bromide.

Statistical analysis

Statistical analysis was performed using GraphPad Prism 6.0 program (Graphpad Software Inc., San Diego, CA, USA). Animal weight, organ weight, and parasite loads were expressed as mean ± standard deviation (SD) of six animals per group. Comparisons of animal weight between groups during infection were analyzed by two-way analysis of variance (ANOVA), followed by the Bonferroni's multiple comparison tests. The difference between weight of uninfected and infected organs was analyzed by Student's *t*-test. Comparisons of parasite loads between groups during infection were analyzed by two-way ANOVA, followed by the Tukey's multiple comparison tests. Differences were considered significant when p values were ≤ 0.05.

Results

Clinical progression of *L. martiniquensis* infection in BALB/c mice and Syrian golden hamsters

Mice and hamsters were experimentally infected with *L. martiniquensis* promastigotes. After *Leishmania* infection, all infected groups reached the study endpoint at 8 and 16 weeks. Over the period of observation, infected BALB/c mice gained their body weight over time and did not lose weight compared to the uninfected group (Fig. 1a). In contrast, infected hamsters only sustained their body weight after infection and began to lose their body weight from 11 weeks post infection onwards. A significant change in the body weight of infected hamsters compared to uninfected controls was observed from week 13 to week 16 (Fig. 1a). No statistically significant differences in the weights of liver and spleen of both 16 weeks-infected BALB/c mice and hamsters compared to uninfected groups were found (Fig. 1b). In infected BALB/c mice, no clinical signs of the disease were found throughout the experiment. However, clinical signs were observed in the infected hamsters in addition to weight loss, these being cachexia and

fatigue, but no ascites, scabs or skin lesions were seen. At necropsy, no changes in colors of the livers and spleens of infected animals were observed (Fig. 1c). No fibrosis was found in any organs. No hepatomegaly and splenomegaly was observed in any infected animals (Fig. 1c).

Presence of *L. martiniquensis* parasites and DNAs in organ tissues of BALB/c mice and Syrian golden hamsters

The liver, spleen, and bone marrow of all infected animals were removed and investigated for *Leishmania* infection. At 8 weeks post infection, no parasites were observed in any impression smears of the liver, spleen, and bone marrow samples of any infected mice or hamsters (data not shown). In contrast, by 16 weeks tissue impression smears of the liver, spleen, and bone marrow of infected hamsters presented numerous intracellular and free amastigotes (Fig. 2d-f), whereas no parasites were seen in tissue smears from the mice at this time point (Fig. 2a-c).

Detection of *L. martiniquensis* DNA using the PCR method was performed on all tissue samples of both infected animals to confirm the impression smear results. PCR results showed that parasite DNAs were detected in the liver and spleen of BALB/c mice, which were negative by impression smears (Fig. 3). In the BALB/c liver tissues, parasite DNAs were detected in five of six infected mice at 8 weeks post infection and one of six infected mice at 16 weeks post infection. For the spleen tissues, parasite DNAs were detected in four of six infected mice at 8 weeks post infection and all infected mice at 16 weeks post infection (Fig. 3). In hamsters infected with *L. martiniquensis*, parasite DNAs were detected in tissues of the liver and spleen of all infected hamsters at 8 and 16 weeks post infection. For the bone marrow samples, parasite DNAs were only detected at 16 weeks post infection in infected hamsters (Fig. 3).

Parasite loads in BALB/c mice and hamsters infected with *L. martiniquensis*

Parasite loads in infected organs were quantified using a limiting dilution assay. At 8 weeks post infection, similar levels of infection were observed in the livers of BALB/c mice (~1×10^3 parasites/gram of organ) and hamsters (~5×10^3 parasites/gram of organ) that were not statistically significantly different (Fig. 4a). However, at 16 weeks post infection, a statistically significant increase of parasite load in the livers of hamsters (~1×10^6 parasites/gram of organ) was noted, whereas the parasite load in the livers of

BALB/c mice (~5×10^2 parasites/gram of organ) did not significantly increase compared to those at 8 weeks post infection (Fig. 4a).

In the spleen, no statistically significant differences in parasite loads were observed between 8 and 16 weeks post infection in BALB/c mice. However, as in the liver, at 16 weeks post infection, parasite load in the spleens of hamsters (1×10^7 parasites/gram of organ) was significantly greater than those at 8 weeks of infection (~5×10^4 parasites/gram of organ) and at 16 weeks post infection in BALB/c mice (~1×10^4 parasites/gram of organ) (Fig. 4b).

Histological alterations in the liver and spleen of infected animals

In infected BALB/c mice no pathological changes in liver and spleen sections after *L. martiniquensis* infection at 8 and 16 weeks were seen (data not shown). Similar results were seen in hamsters at 8 weeks post infection (data not shown). However, for hamsters, alterations of the infected liver were seen at 16 weeks post infection with large areas of necrosis (Fig. 5b). Compared to normal liver tissue of the uninfected hamsters (Fig. 5a) cellular infiltrates of macrophages and lymphocytes were observed in the perivascular region (Fig. 5b). Also, compared to normal hepatocytes of the uninfected liver (Fig. 5c) nuclear destruction and cytoplasmic degeneration of the infected hepatocytes and the presence of amastigotes of *L. martiniquensis* were found in the infected tissue (Fig. 5d). Changes in splenic architecture were presented in the infected spleen. Reduction and deformation of white pulp compared to those of uninfected control were noted (Fig. 5e and 5f). Compared to the normal white pulp of the uninfected spleen (Fig. 1g), in the infected spleen, clusters of macrophages and numerous amastigotes were found (Fig. 5h).

Discussion

Experimental infections with *L. martiniquensis* in BALB/c mice and Syrian golden hamsters were performed to investigate an appropriate animal model for this *Leishmania* species. Mice and hamsters were injected intraperitoneally with promastigotes of *L. martiniquensis* and then monitored for 16 weeks. In this study, the infected BALB/c mice were clinically asymptomatic, whereas the infected hamsters developed symptomatic infection after 11 weeks post infection, presenting with weight loss, cachexia and fatigue. No hepatomegaly and splenomegaly were found in either mice or hamsters. Hepatomegaly and

splenomegaly are common in visceral leishmaniasis, however, most models of murine infection exhibit the subclinical or asymptomatic form of visceral leishmaniasis (Aslan et al. 2013; Gomes-Silva et al. 2013; Martín-Martín et al. 2015; McCall et al. 2013). The splenomegaly could appear in BALB/c mice depending on the inoculum size (de Melo et al. 2020). Hamsters infected with *L. infantum* present splenomegaly after 3 months post-infection being more evident at 6 and 9 months after the infection (Moreira et al. 2016).

Although the macroscopic examinations of the liver and spleen of infected hamsters were normal, numerous amastigotes were found in tissue impression smears of all examined organs of the infected hamsters at week16 of infection. These results indicate that *L. martiniquensis* parasites were able to infect the liver and spleen of hamsters and disseminated to their bone marrow, which correlated with the severity of infection. However, in BALB/c mice, amastigotes were not found in the tissue impression smears examined, but parasite DNAs were detected in the liver and spleen tissues, suggesting that the PCR method was more appropriate for detection of these low numbers of amastigotes in the organ tissues than the microscopic method. PCR based methods have been used to detect *Leishmania* parasite in several studies as they have provided high sensitivity, accuracy, and reproducibility (Solotra et al. 2001; Pothirat et al. 2014; Chiewchanvit et al. 2015; Ranasinghe et al. 2015; Montalvo et al. 2017; Medkour et al. 2020).

L. martiniquensis DNAs were detected in tissues of mice and hamsters at various points. For BALB/c mice, parasite DNAs were detected in the liver at week 8 of infection, followed by nearly clearance of parasites in week 16, whereas in the spleen parasite DNAs were detected in all animals at 16 weeks of infection. No parasite DNA was detected in the bone marrow of mice at any time point indicating that no dissemination of parasites to the bone marrow occurred. These results suggest the control of visceralization of *L. martiniquensis* in BALB/c mice. Another reason might be due to the period of the infection course in this study. Evaluation of parasite persistence and visceralization in BALB/c mice might need a longer infection course.

Garin et al (2001) have monitored the infection of two strains of a presumed lower trypanosomatid (later identified as *L. martiniquensis* by Desbois et al (2014)) isolated from an HIV-infected patient (MHOM/MQ/92/MARl) and an immunocompetent patient (MHOM/MQ/97/MAR2) in BALB/c mice for 150 days via subcutaneous and intravenous inoculation with 10^7 promastigotes. At day 150, parasites are

observed in liver, spleen, foot pad, popliteal, and mesenteric lymph nodes in mice infected with MHOM/MQ/92/MARl promastigotes via subcutaneous inoculation. In mice infected with MHOM/MQ/92/MARl promastigotes via intravenous inoculation, parasites are found in liver, spleen, mesenteric lymph node, and brain. For mice infected with MHOM/MQ/92/MAR2 parasites via subcutaneous inoculation, at day 150, parasites are found only in foot pad and popliteal lymph node but via intravenous inoculation parasites are observed in liver, spleen, and mesenteric lymph node. At all time point of infection, no parasites are observed in liver and spleen of BALB/c mice infected with MHOM/MQ/92/MAR2 parasites via subcutaneous inoculation, whereas mice infected with the same strain via intravenous inoculation, parasites are observed in both organs. In our study, the BALB/c mice were intraperitoneally injected with 2×10^7 *L. martiniquensis* (MHOM/TH/2013/LSCM3) promastigotes and parasites were detected in liver and spleen at all time point of the infection. Recently, the study of the infection of *L. martiniquensis* (MHOM/TH/2011/PG) in BALB/c mice has shown that, after intravenous inoculation and intraperitoneal inoculation with 5×10^6 promastigotes, parasite DNAs are detected in the bone marrow at 16 weeks post-infection (Somboonpoonpol 2016). In the present study, no *L. martiniquensis* (MHOM/TH/2013/LSCM3) DNAs were found in bone marrow at the same time point of the infection. These results suggest that several factors such as parasite strain, inoculum size and inoculation route influence the outcome of visceral leishmaniasis caused by *L. martiniquensis* in BALB/c mice.

From experimental data on *L. infantum* infection in BALB/c mice reviewed by Loeuillet et al (2016), elimination of parasites in the liver and their persistence in the spleen involves organ-specific immune responses. In the early stage of infection, *L. infantum* promastigotes are rapidly cleared (more than 95%) from the circulation of infected BALB/c mice via phagocytosis by marginal zone macrophages in spleen. In the liver, *L. infantum* promastigotes invade the resident macrophages, Kupffer cells and dendritic cells, becoming amastigotes and replicating. In the first two weeks, in liver, TGFβ (macrophage-inhibitory cytokines) levels are elevated. TGFβ produced by cells of the spleen red pulp may contribute to the establishment of infection and parasite replication. In addition, a Th1 immune response inducing macrophages to synthesize leishmanicidal molecules, such as nitric oxide (NO) is ineffective. Both elevated TGFβ levels and ineffective Th1 response allow uncontrolled parasite growth. In the spleen, in the first four weeks, immune cells, such as $CD4^+$ T, $CD8^+$ T and natural killer (NK) cells, are not capable

of producing IFNγ and IL2 (macrophage-activating cytokines) that promote NO synthesis. After the first 4 weeks of infection, the immune cells recover their capacity to produce IFNγ, thus promoting leishmanicidal activity of the macrophages with NO synthesis and control of granuloma formation (parasitized Kupffer cells) in the liver. Thus, parasite burden reduces ultimately. In synergy with IFNγ, IL17A also contributes to macrophage activation with NO production, leading to parasite clearance. In liver, infection is resolved after 8 weeks of infection. However, in the spleen, infection is maintained during the entire visceral leishmaniasis course. *L. infantum* parasite persistence may be due to sustained TGFβ production by $CD4^+$ $CD25^+$ T cells that contributes to immunosuppression (Rodrigues et al. 2009). The control of visceralization of *L. martiniquensis* infection in BALB/c mice might use similar immune control of infection as in *L. infantum*.

In hamsters, *L. martiniquensis* parasites grew and persisted in the liver, spleen, and bone marrow over the period of infection suggesting this animal is a suitable experimental model for study of pathological features of visceral leishmaniasis caused by *L. martiniquensis*. A possible explanation for the suitability of this experimental model might be similar to that seen in experimental studies in *L. infantum* and *L. donovani*-infected hamsters, where early production of IL10 and TGFβ and the impairment of NO synthesis in response to IFN_Υ contribute to establishing of *Leishmania* infection and defective parasite killing (Melby et al. 2001; Nieto et al. 2011). However, more studies of cytokine production kinetics and activation of the different classes of immune cells by *L. martiniquensis* infection in both BALB/c mice and hamsters are required.

Considering parasite load, which indicates the growth capacity of parasites in animal organs, we observed that growth of *L. martiniquensis* parasites was limited in the tissues of BALB/c mice. Parasite numbers had not increased in liver and spleen at 16 weeks of infection compared to 8 weeks. In contrast, in hamsters, parasites had significantly increased in number by 16 weeks of infection in both liver and spleen. These results correlate with those on the presence of parasites in tissue smears and DNAs in the examined organs. It is possible that the high parasite growth induced an inflammatory response and the resulting pathological changes observed in the organ tissues of hamsters.

Hamsters infected with *L. martiniquensis* had significant changes in the liver and spleen tissues. Alterations in the liver with necrosis of hepatocytes appeared to be a consequence of amastigote infection. The presence of inflammatory infiltrates consisting of macrophages and lymphocytes accumulating

around the portal vein was similar to several studies on visceral leishmaniasis (Gomes-Silva et al. 2013; Rashidi et al. 2018). Inflammatory infiltrates indicate a chronic hepatitis due to *Leishmania* infection. The Kupffer cells containing parasites in their cytoplasm develop a progressive cellular swelling, nuclear degeneration and disruption of plasma membrane (González et al. 1988; Vianna et al. 2002). Infection by *L. martiniquensis* parasites changed the morphology of splenic pulps, and also reduction and deformation of white pulp in the spleen of infected hamsters were observed. This is similar to the data reviewed by Hermida et al (2018) that white pulp atrophy, disappearance of secondary lymphoid follicles and the marginal zone, and morphological alterations of the red and white pulps are associated with the chronic severe form of visceral leishmaniasis in dogs infected with *L. infantum*.

In conclusion, this work examined the infection of *L. martiniquensis* in BALB/c mice and Syrian golden hamsters, with regard to clinical presentation, visceralization and proliferation of parasites, and histological alterations in the organ tissues. During the course of infection no clinical signs were observed in BALB/c mice. Parasite DNAs were detected in the liver at week 8 of infection, but cleared in most animals at week 16, whereas parasite DNA was detected in the spleen until week 16 of infection. These results are correlated with the results of parasite loads in the liver and spleen. No dissemination to the bone marrow occurred and no alterations in the tissues of the BALB/c mice were observed. However, extension of the period of infection up to 1 year for BALB/c mice could provide more information regarding clinical manifestations, pathological changes in tissues/organs, and biochemical/hematological alterations. For Syrian golden hamsters, weight loss, cachexia and fatigue were observed after 11 weeks of infection. *L. martiniquensis* parasites infected both liver and spleen and disseminated to bone marrow. Parasite loads correlated with the results of presence of parasites and DNAs in liver and spleen. At week 16 of infection, hamsters infected with *L. martiniquensis* exhibited signficant histological alterations in the liver and spleen tissues indicating progressive visceral leishmaniasis. Therefore, the Syrian golden hamster is an appropriate animal model for study of pathological features of chronic visceral leishmaniasis caused by *L. martiniquensis*.

Acknowledgements

We thank Prof. Dr. Padet Siriyasatein and Assist. Prof. Dr. Woraporn Sukhumavasi for their suggestion in the route of experimental infection.

Funding

This research work was supported by the Thailand Research Fund through the Royal Golden Jubilee Ph.D. Program (grant number: PHD/0100/2557 to NJ for NI), the Faculty of Medicine Endowment Fund (grant number: 161-2561 to NJ) from the Faculty of Medicine, Chiang Mai University and Global Partnership Fund year 2020, supported by The Thailand Science Research and Innovation (TSRI) (grant number 2563 subproject to NJ).

Compliance with ethical standards

Conflict of interests

The authors declare that they have no conflict of interests.

Author contributions

NJ conceived and designed study. NI, WC and AK performed research. NJ, NI, PS, and MDB analyzed data. NJ, NI and PAB wrote the paper. All authors read and approved the final version of the manuscript.

References

Aslan H, Dey R, Meneses C, Castrovinci P, Jeronimo SM, Oliva G, Fischer L, Duncan RC, Nakhasi HL, Valenzuela JG, Kamhawi S (2013) A new model of progressive visceral leishmaniasis in hamsters by natural transmission via bites of vector sand flies. J Infect Dis 207:1328-1338

Becvar T, Siriyasatien P, Bates PA, Volf P, Sádlová J (2020) Development of *Leishmania* (*Mundinia*) in guinea pigs. Parasit Vectors 13:181

Buffet PA, Sulahian A, Garin YJ, Nassar N, Derouin F (1995) Culture microtitration: a sensitive method for quantifying *Leishmania infantum* in tissues of infected mice. Antimicrob Agents and Chemother 39:2167-2168

Carrion J, Nieto A, Iborra S, Iniesta V, Soto M, Folgueira C, Abanades DR, Requena JM, Alonso C (2006) Immunohistological features of visceral leishmaniasis in BALB/c mice. Parasite Immunol 28:173-183

Chiewchanvit S, Tovanabutra N, Jariyapan N, Bates MD, Mahanupab P, Chuamanochan M, Tantiworawit A, Bates PA (2015) Chronic generalized fibrotic skin lesions from disseminated leishmaniasis caused by *Leishmania martiniquensis* in two patients from northern Thailand infected with HIV. Br. J. Dermatol 173:663-670

de Melo CVB, Hermida MD, Mesquita BA, Fontes JLM, Koning JJ, Solcà MDS, Benevides BB, Mota GBS, Freitas LAR, Mebius RE, Dos-Santos WLC (2020) Phenotypical characterization of spleen remodeling in murine experimental visceral leishmaniasis. Front Immunol 11:653

Desbois N, Pratlong F, Quist D, Dedet JP (2014) *Leishmania* (*Leishmania*) *martiniquensis* n. sp. (Kinetoplastida: Trypanosomatidae), description of the parasite responsible for cutaneous leishmaniasis in Martinique Island (French West Indies). Parasite 21:12

Garin YJ, Sulahian A, Méneceur P, Pratlong F, Prina E, Gangneux J, Dedet JP, Derouin F (2001) Experimental pathogenicity of a presumed monoxenous Trypanosomatid isolated from humans in a murine model. J Eukaryot Microbiol 48:170-176

Gomes-Silva A, Valverde JG, Ribeiro-Romão RP, Plácido-Pereira RM, Da-Cruz AM (2013) Golden hamster (*Mesocricetus auratus*) as an experimental model for *Leishmania* (*Viannia*) *braziliensis* infection. Parasitology 140, 771-779

González JL, Rollán E, Novoa C, Castaño M (1988) Structural and ultrastructural hepatic changes in experimental canine leishmaniasis. Histol Histopathol 3:323-329

Gupta R, Kushawaha PK, Samant M, Jaiswal AK, Baharia RK, Dube A (2012) Treatment of *Leishmania donovani*-infected hamsters with miltefosine: analysis of cytokine mRNA expression by real-time PCR, lymphoproliferation, nitrite production and antibody responses. J Antimicrob Chemother 67:440-443

Handman E (2001) Leishmaniasis: current status of vaccine development. Clin Microbiol Rev 14:229-243

Hermida MD, de Melo CVB, Lima IDS, Oliveira GGS, Dos-Santos WLC (2018) Histological disorganization of spleen compartments and severe visceral leishmaniasis. Front Cell Infect Microbiol 8:394

Jariyapan N, Daroontum T, Jaiwong K, Chanmol W, Intakhan N, Sor-Suwan S, Siriyasatien P, Somboon P, Bates MD, Bates PA (2018) *Leishmania* (*Mundinia*) *orientalis* n. sp. (Trypanosomatidae), a parasite from Thailand responsible for localised cutaneous leishmaniasis. Parasit Vector 11:351

Johnson M (2012) Laboratory mice and rats. Mater Methods 2:113

Leelayoova S, Siripattanapipong S, Manomat J, Piyaraj P, Tan-Ariya P, Bualert L, Mungthin M (2017) Leishmaniasis in Thailand: A review of causative agents and situations. Am J Trop Med Hyg 96:534-542

Loeuillet C, Bañuls AL, Hide M (2016) Study of *Leishmania* pathogenesis in mice: experimental considerations. Parasit Vectors 9:144

Loría-Cervera EN, Andrade-Narváez FJ (2014) Animal models for the study of leishmaniasis immunology. Rev Inst Med Trop Sao Paulo 56:1-11

Martín-Martín I, Jiménez M, González E, Eguiluz C, Molina R (2015) Natural transmission of *Leishmania infantum* through experimentally infected *Phlebotomus perniciosus* highlights the virulence of *Leishmania* parasites circulating in the human visceral leishmaniasis outbreak in Madrid, Spain. Vet Res 46:138

McCall LI, Zhang WW, Matlashewski G (2013) Determinants for the development of visceral leishmaniasis disease. PLoS Pathog 9:e1003053

Medkour H, Laidoudi Y, Athias E, Bouam A, Dizoé S, Davoust B, Mediannikov O (2020) Molecular and serological detection of animal and human vector-born pathogens in the blood of dogs from Côte d'lvoire. Comp Immunol Microbiol Infect Dis 69:101412

Melby PC, Chandrasekar B, Zhao W, Coe JE (2001) The hamster as a model of human visceral leishmaniasis: progressive disease and impaired generation of nitric oxide in the face of a prominent Th1-like cytokine response. J Immunol 166:1912-1920

Montalvo AM, Fraga J, Tirado D, Blandón G, Alba A, Van der Auwera G, Vélez ID, Muskus C (2017) Detection and identification of *Leishmania* spp.: application of two hsp70-based PCR-RFLP protocols to clinical samples from the new world. Parasitol Res 116:1843-1848

Moreira Nd, Vitoriano-Souza J, Roatt BM, Vieira PM, Coura-Vital W, Cardoso JM, Rezende MT, Ker HG, Giunchetti RC, Carneiro CM, Reis AB (2016) Clinical, hematological and biochemical alterations in hamster (*Mesocricetus auratus*) experimentally infected with *Leishmania infantum* through different routes of inoculation. Parasit Vectors 9:181

Nieto A, Domínguez-Beral G, Orden JA, De La Fuente R, Madrid-Elena N, Carrión J (2011) Mechanisms of resistance and susceptibility to experimental visceral leishmaniasis: BALB/c mouse versus

463 Syrian hamster model. Vet Res 42:39
464 Ong HB, Clare S, Roberts AJ, Wilson ME, Wright GJ (2020) Establishment, optimisation and
465 quantitation of a bioluminescent murine infection model of visceral leishmaniasis for systematic
466 vaccine screening. Sci Rep 10:4689
467 Pothirat T, Tantiworawit A, Chaiwarith R, Jariyapan N, Wannasan A, Siriyasatien P, Supparatpinyo K,
468 Bates MD, Kwakye-Nuako G, Bates PA (2014) First isolation of *Leishmania* from Northern
469 Thailand: case report, identification as *Leishmania martiniquensis* and phylogenetic position
470 within the *Leishmania enriettii* complex. PLoS Negl Trop Dis 8:e3339
471 Rashidi S, Kalantar K, Hatam G (2018) Achievement amastigotes of *Leishmania infantum* and
472 investigation of pathological changes in the tissues of infected golden hamsters. J Parasit Dis
473 42:187-195
474 Ranasinghe S, Wickremasinghe R, Hulangamuwa S, Sirimanna G, Opathella N, Maingon RD,
475 Chandrasekharan V (2015) Polymerase chain reaction detection of *Leishmania* DNA in skin
476 biopsy samples in Sri Lanka where the causative agent of cutaneous leishmaniasis in *Leishmania*
477 *donovani*. Mem Inst Oswaldo Cruz 110:1017-1023
478 Robledo SM, Carrillo LM, Daza A, Restrepo AM, Muñoz DL, Tobón J, Murillo JD, López A, Ríos C,
479 Mesa CV, Upegui YA, Valencia-Tobón A, Mondragón-Shem K, Rodríguez B, Vélez ID (2012)
480 Cutaneous leishmaniasis in the dorsal skin of hamsters: a useful model for the screening of
481 antileishmanial drugs. J Vis Exp 62:3533
482 Rodrigues,OR, Marques C, Soares-Clemente M, Ferronha MH, Santos-Gomes GM (2009) Identification
483 of regulatory T cells during experimental *Leishmania infantum* infection. Immunobiology
484 214:101-111
485 Solotra P, Sreenivas G, Pogue GP, Lee N, Nakhasi HL, Ramesh V, Negi NS (2001) Development of a
486 species-specific PCR assay for detection of *Leishmania donovani* in clinical samples from
487 patients with kala-azar and post-kala-azar demal leishmaniasis. J Clin Microbiol 39:849-854
488 Somboonpoonpol N (2016) Parasite burden, distribution and immunopathology of *Leishmania*
489 *martiniquensis* - infected BALB/c mice in different routes and time points.
490 http://cuir.car.chula.ac.th/handle/123456789/60706 (accessed 18 April 2020)
491 Spanakos G, Piperaki ET, Menounos PG, Tegos N, Flemetakis A, Vakalis NC (2008) Detection and

492 species identification of Old World *Leishmania* in clinical samples using a PCR-based method.
493 Trans R Soc Trop Med Hyg 102:46-53
494 Vianna VL, Takiya CM, de Brito-Gitirana L (2002) Histopathologic analysis of hamster hepatocytes
495 submitted to experimental infection with *Leishmania donovani*. Parasitol Res. 88:829-836
496 WHO 2019 Leishmaniasis. https://wwwwhoint/news-room/fact-sheets/detail/leishmaniasis.
497 Zakai HA, Chance ML, Bates PA (1998) *In vitro* stimulation of metacyclogenesis in *Leishmania*
498 *braziliensis, L. donovani, L. major* and *L. mexicana*. Parasitology 116:305-309
499

500 **Figure captions**

501 **Fig. 1** Comparative clinicopathology of *L. martiniquensis* infection in BALB/c and Syrian golden
502 hamsters. **a** Body weights of infected mice and hamsters compared to uninfected groups over time of
503 infection. **b** Liver (left bar) and spleen (right bar) weights of 16 weeks-infected mice and hamsters
504 compared with uninfected group. Results are expressed as mean ± SD. **c** Macroscopic aspect of infected
505 and uninfected animals, infected livers, and infected spleens compared to uninfected organs. Bar = 1 cm
506

507 **Fig. 2** Light micrographs of Giemsa-stained imprints from the liver and spleen of BALB/c mice and
508 Syrian golden hamsters after 16 weeks post infection. **a** Liver, **b** spleen, and **c** bone marrow impression
509 smears of mice. **d** liver, **e** spleen, and **f** bone marrow impression smears of hamsters. Arrows indicate
510 amastigotes of *L. martiniquensis*. Bar: 20 μm
511

512 **Fig. 3** PCR amplification of *L. martiniquensis* DNAs in tissue samples of BALB/c mice and Syrian
513 golden hamsters using LeF/LeR primers for *Leishmania* rRNA ITS-1. Tissues of animals were sampled at
514 8 and 16 weeks post infection (w pi.). Lanes: MW, 100 bp DNA ladder; Neg, negative control - no DNA;
515 Pos, positive control - *L. martiniquensis* DNA; **a-f**, samples from mice; **g-l**, samples from hamsters. BM -
516 bone marrow
517

518 **Fig. 4** Parasite loads in the livers and spleens of BALB/c mice and Syrian golden hamsters infected with
519 *L. martiniquensis* determined by limiting dilution assay. **a** Parasite load quantified from the liver of
520 infected mice and hamsters at 8 and 16 weeks post infection. **b** Parasite load quantified from the spleens

of infected mice and hamsters at 8 and 16 weeks post infection. Results are expressed as mean ± SD of six animals per group. White bar: BALB/c. Black bar: hamster. $^{**}p \leq 0.001$, $^{****}p \leq 0.0001$

Fig. 5 Histological sections of the liver and spleen of *L. martiniquensis*-infected hamsters compared with uninfected controls. **a** Normal tissue of the uninfected liver with normal cellular organization. **b** Mononuclear infiltrates in perivascular region and tissue alterations found in the infected liver. **c** Normal hepatocytes of the uninfected liver. **d** Degenerating hepatocytes of the infected liver showing non-nucleated cells. Arrows indicate cells containing amastigotes inside. **e** Normal architecture of the uninfected spleen with distinction between the white and red pulp. **f** Deformation and reduction of the white pulp of the infected spleen. **g** Normal white pulp of the uninfected spleen. **h** Clusters of macrophages containing numerous amastigotes inside (arrows) found in the infected spleen. PV: portal vein, WP: white pulp. **a**, **b**, **e** and **f**, Bar: 200 μm. **c**, **d**, **g** and **h**, Bar = Bar: 20 μm

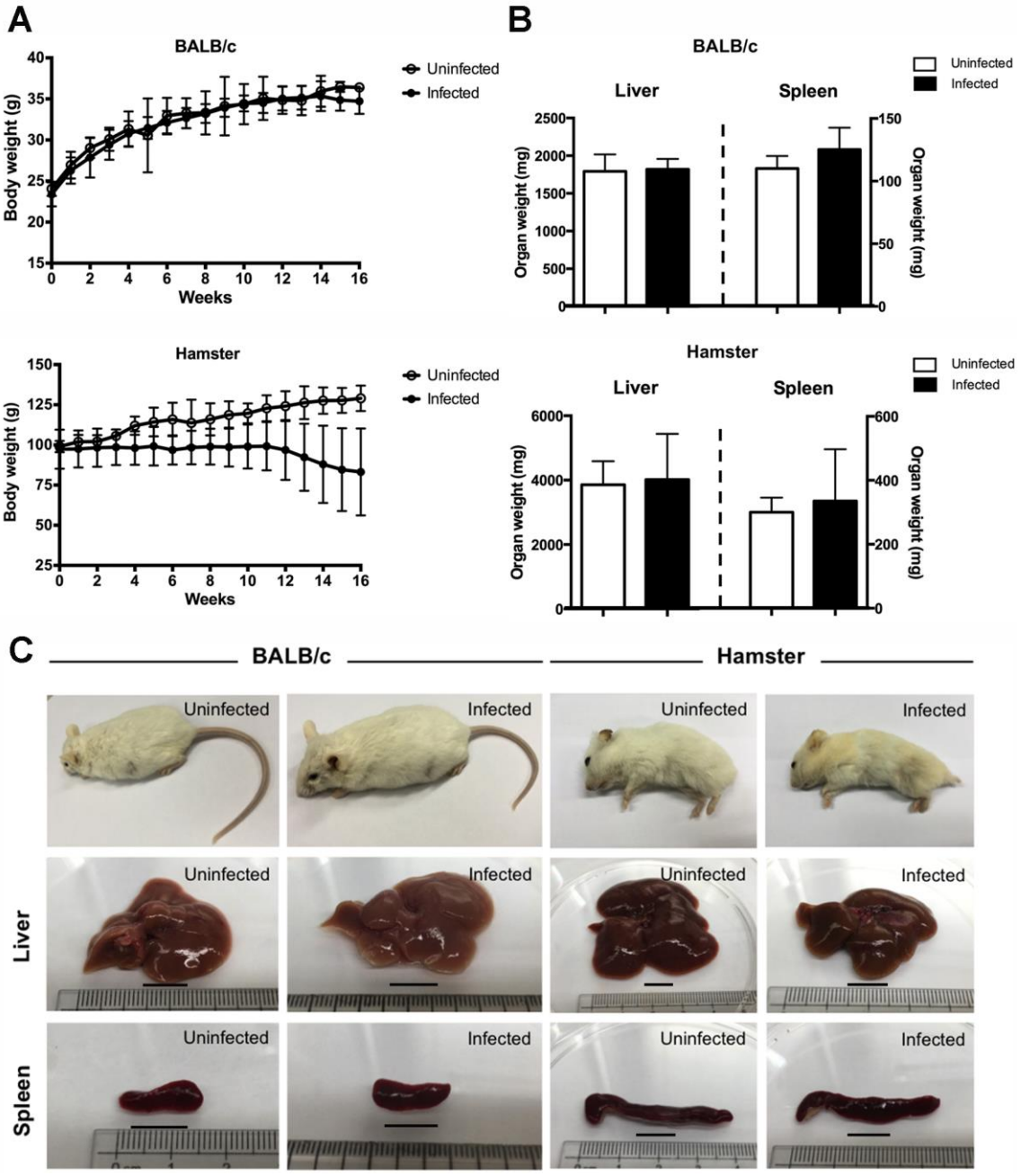

533

534 Figure 1.

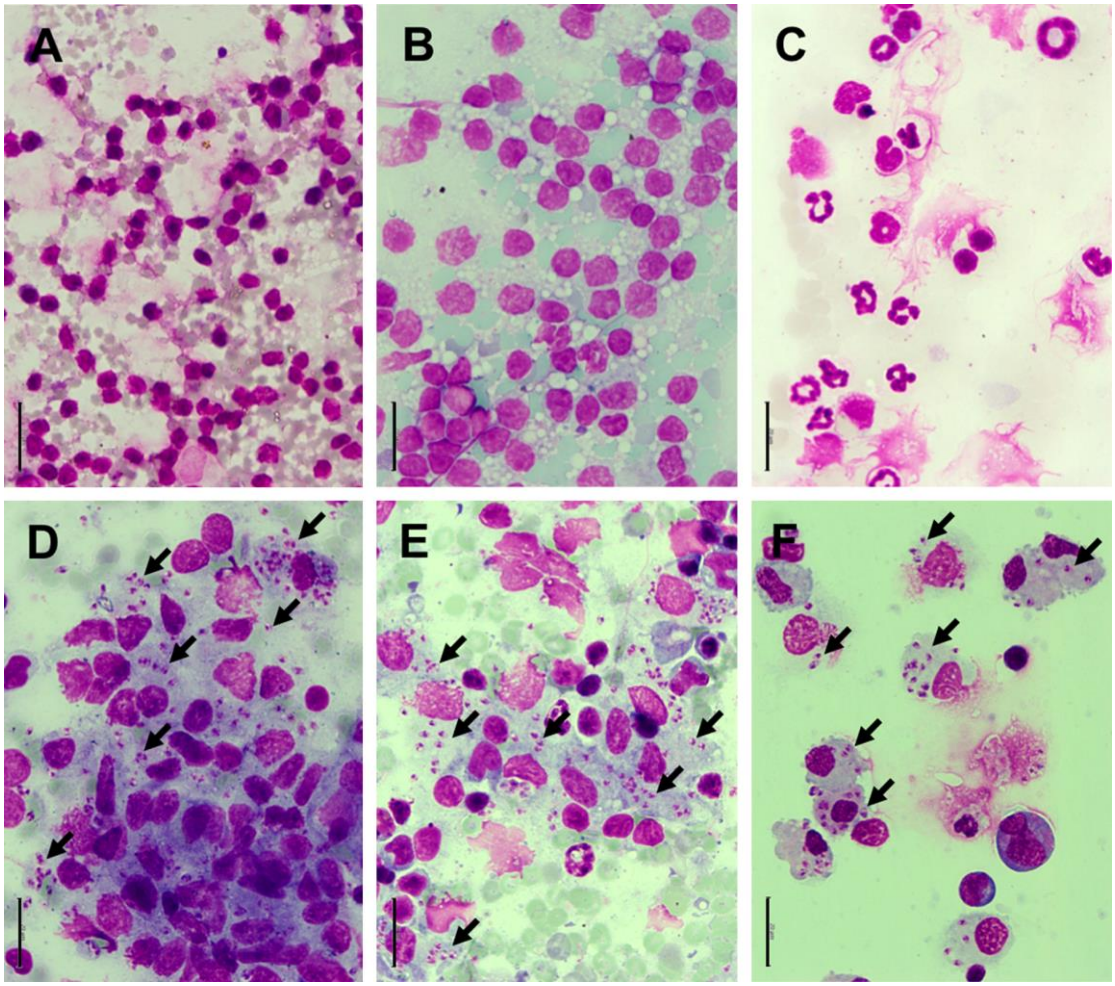

Figure 2.

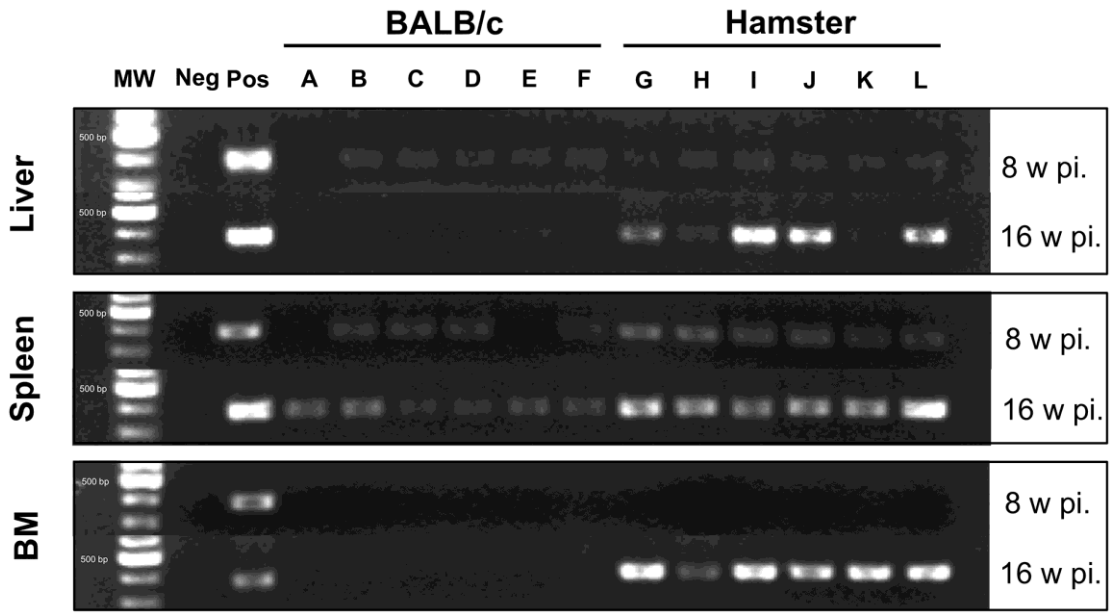

Figure 3.

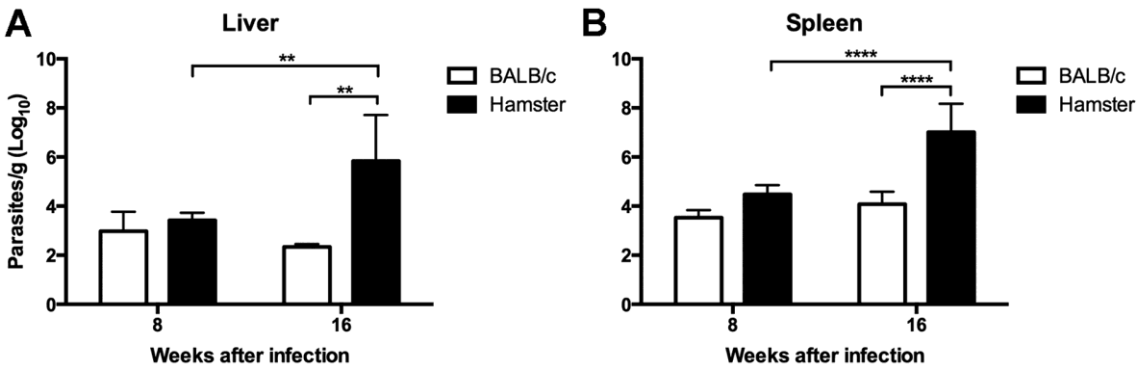

539

540 Figure 4.

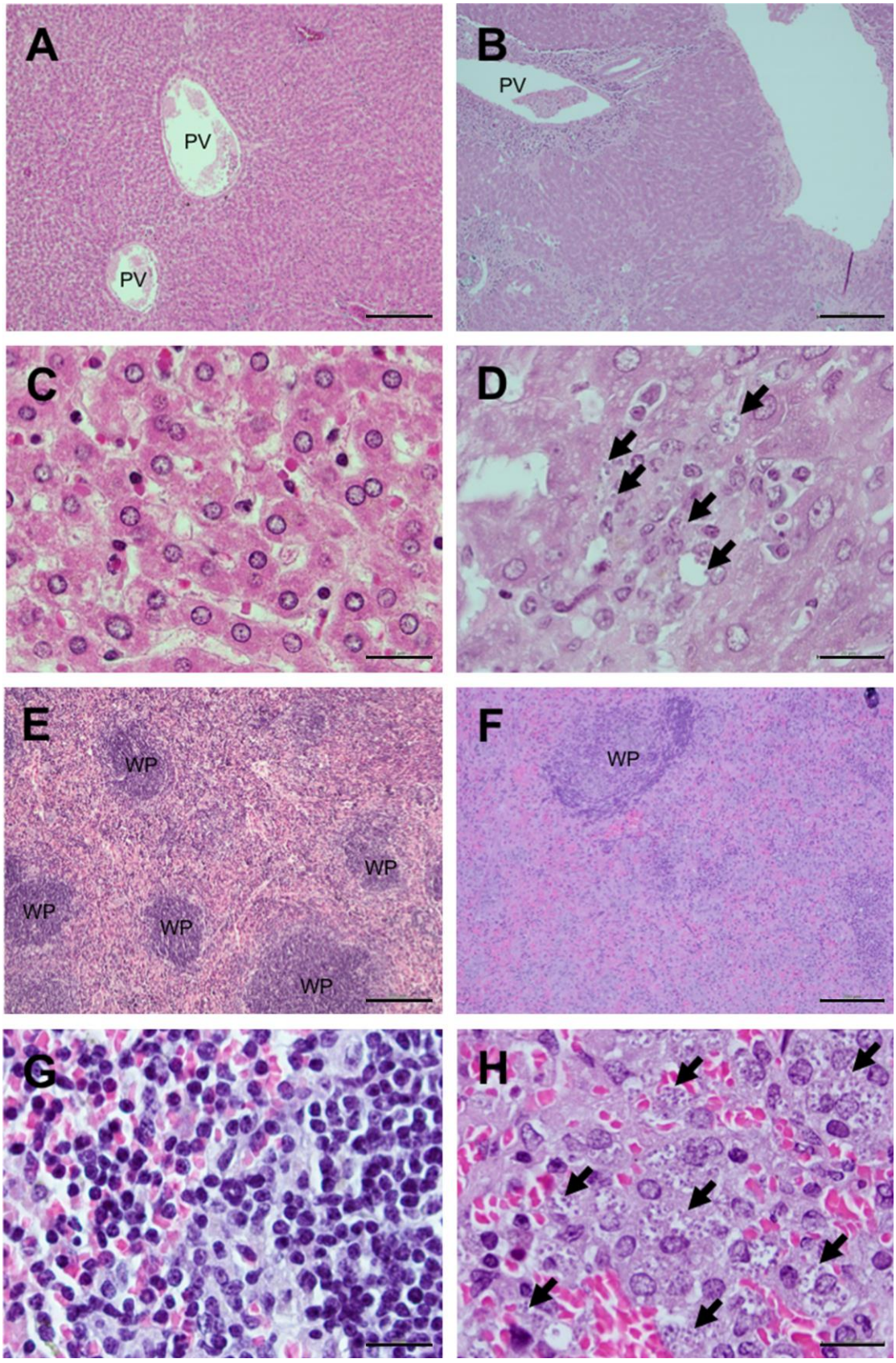

Figure 5.